Spectroscopy Results from COMPASS

Jan Friedrich

Physik-Department, TU München
on behalf of the COMPASS collaboration

11th European Research Conference on
"Electromagnetic Interactions with Nucleons and Nuclei"
EINN2015, 5. November
Πάφος, Κύπρος

COMPASS MLL TUM LMU ESO

Bundesministerium
für Bildung
und Forschung

NIMA **779** (2015) 69

Fixed-target experiment

- Two-stage spectrometer
- Large acceptance over wide kinematic range
- Electromagnetic and hadronic calorimeters
- Beam and final-state particle ID (CEDARs, RICH)

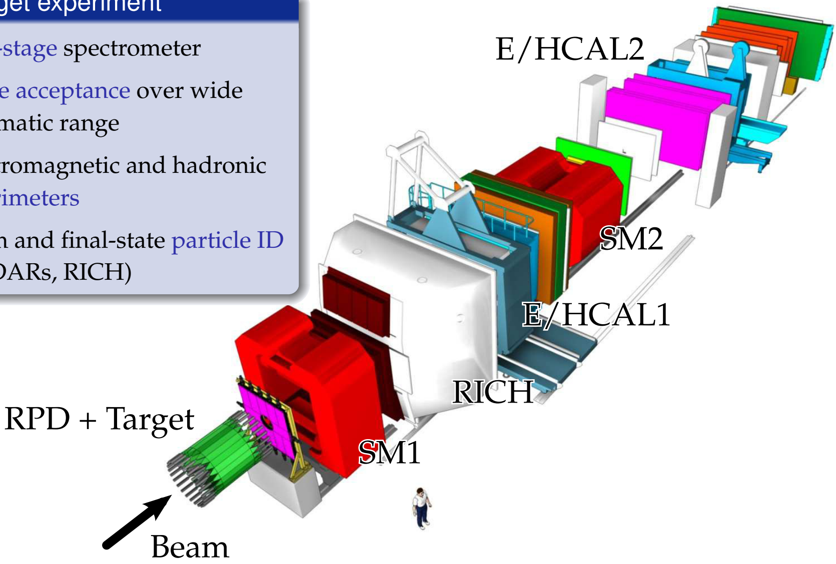

The COMPASS Experiment at the CERN SPS

Experimental Setup

NIMA **779** (2015) 69

Fixed-target experiment

- Two-stage spectrometer
- Large acceptance over wide kinematic range
- Electromagnetic and hadronic calorimeters
- Beam and final-state particle ID (CEDARs, RICH)

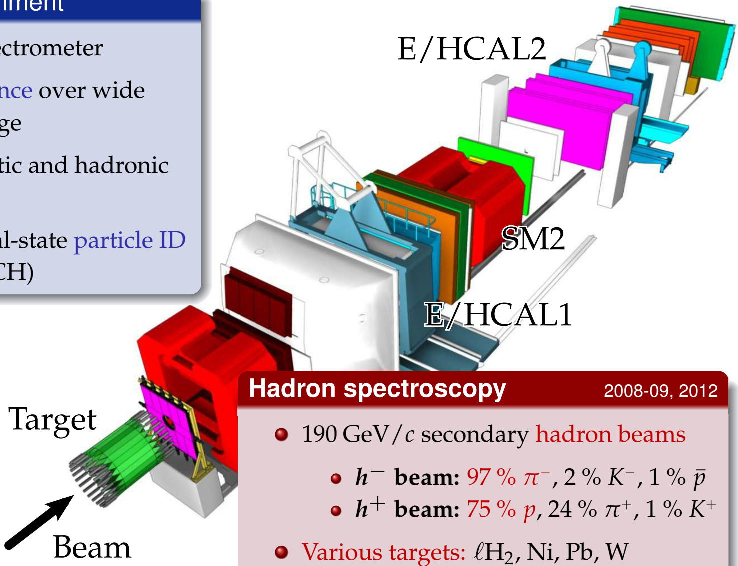

Hadron spectroscopy 2008-09, 2012

- 190 GeV/c secondary hadron beams
  - h^- **beam:** 97 % π^-, 2 % K^-, 1 % $\bar{p}$
  - h^+ **beam:** 75 % p, 24 % π^+, 1 % K^+
- Various targets: ℓH_2, Ni, Pb, W

NIMA **779** (2015) 69

Fixed-target experiment

- Two-stage spectrometer
- Large acceptance over wide kinematic range
- Electromagnetic and hadronic calorimeters
- Beam and final-state particle ID (CEDARs, RICH)

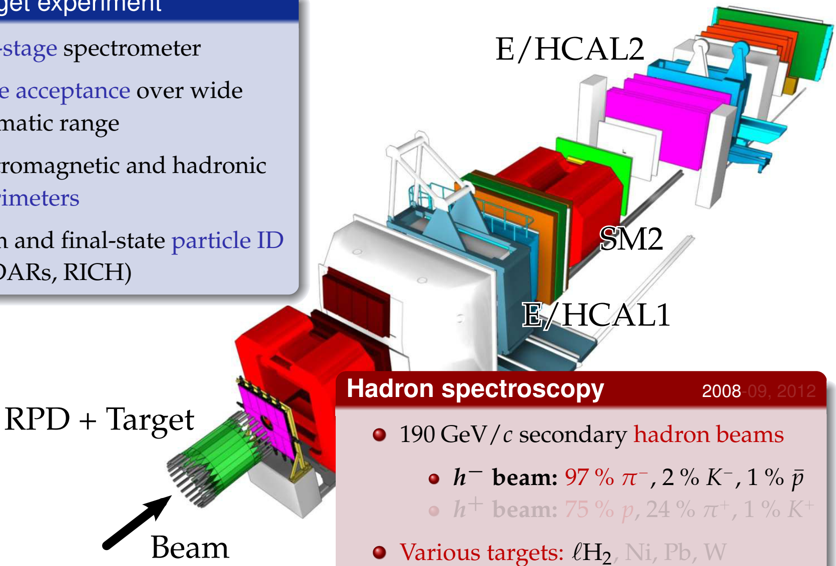

Hadron spectroscopy 2008-09, 2012

- 190 GeV/c secondary hadron beams
  - h^- **beam:** 97 % π^-, 2 % K^-, 1 % $\bar{p}$
  - h^+ **beam:** 75 % p, 24 % π^+, 1 % K^+
- Various targets: ℓH_2, Ni, Pb, W

NIMA **779** (2015) 69

Spectroscopy program

- Explore light-meson spectrum, extending to $m \gtrsim 2\ \mathrm{GeV}/c^2$
- Search for states beyond the constituent quark model
- Precision measurement of known resonances

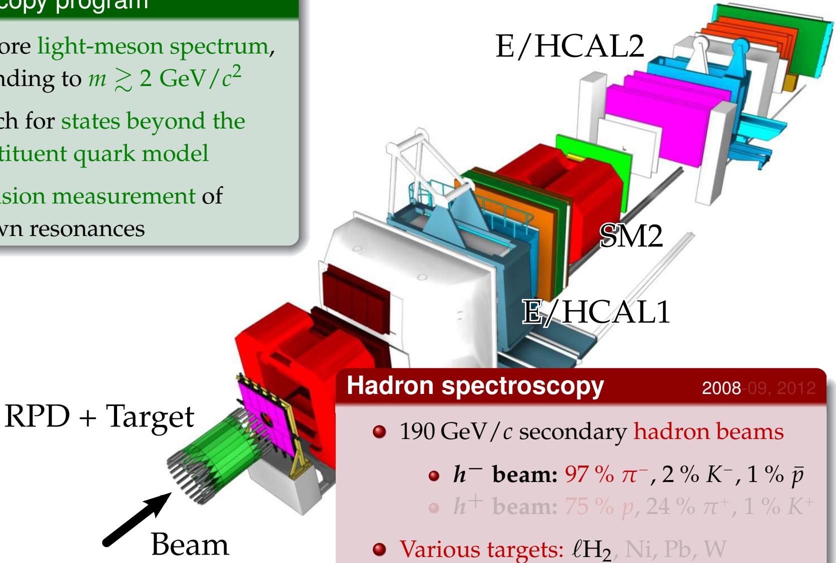

Hadron spectroscopy 2008-09, 2012

- 190 GeV/c secondary hadron beams
  - h^- **beam:** 97 % π^-, 2 % K^-, 1 % $\bar{p}$
  - h^+ **beam:** 75 % p, 24 % π^+, 1 % K^+
- Various targets: ℓH_2, Ni, Pb, W

Outline

1. Introduction
   - Meson production in diffractive dissociation
   - Partial-wave analysis method
2. PWA of diffractively produced $\pi^-\eta$ and $\pi^-\eta'$ final states
   - Even partial waves similar
   - Exotic 1^{-+} much stronger in $\pi^-\eta'$
3. PWA of diffractively produced 3π final states
   - Observation of a new narrow axial-vector meson $a_1(1420)$
   - $J^{PC} = 1^{-+}$ spin-exotic partial wave
4. Conclusions and outlook

Outline

1. Introduction
   - Meson production in diffractive dissociation
   - Partial-wave analysis method
2. PWA of diffractively produced $\pi^-\eta$ and $\pi^-\eta'$ final states
   - Even partial waves similar
   - Exotic 1^{-+} much stronger in $\pi^-\eta'$
3. PWA of diffractively produced 3π final states
   - Observation of a new narrow axial-vector meson $a_1(1420)$
   - $J^{PC} = 1^{-+}$ spin-exotic partial wave
4. Conclusions and outlook

Meson Production in Diffractive Dissociation

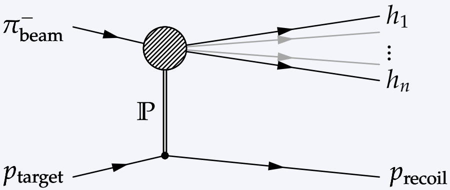

- Beam particle gets excited into intermediate resonances X
- X dissociate into n-body final state
- Rich spectrum of intermediate states X

Disentanglement of all contributing X by **partial-wave analysis** (PWA)

Meson Production in Diffractive Dissociation

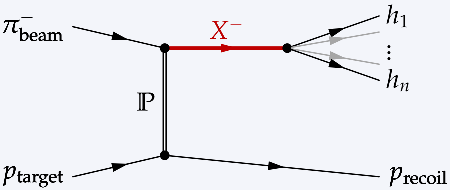

- Beam particle gets excited into intermediate resonances X
- X dissociate into n-body final state
- Rich spectrum of intermediate states X

Disentanglement of all contributing X by **partial-wave analysis** (PWA)

Meson Production in Diffractive Dissociation

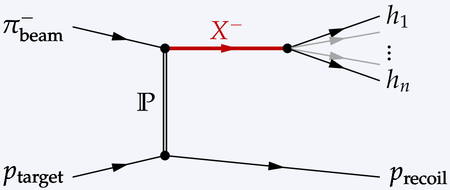

- Beam particle gets excited into intermediate resonances X
- X dissociate into n-body final state
- Rich spectrum of intermediate states X

Disentanglement of all contributing X by **partial-wave analysis** (PWA)

Partial-Wave Analysis Method

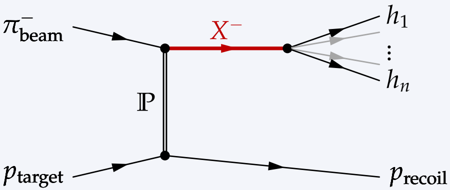

Two-stage analysis

$$\sigma(\tau; m_X) \propto \sum_{\epsilon=\pm1} \left| \sum_i^{\text{waves}} T_i^\epsilon(m_X)\, A_i^\epsilon(\tau; m_X) \right|^2$$

1. **Determination of m_X dependence of spin-density matrix $\varrho_{ij}^\epsilon(m_X) = T_i^\epsilon(m_X)\, T_j^{\epsilon *}(m_X)$**
   - Independent maximum likelihood fits to τ distributions in narrow m_X bins
   - Take into account detection efficiency
   - No assumptions about resonance content of X
2. **Extraction of resonances**
   - χ^2 fit of resonance model to spin-density (sub)matrix

Partial-Wave Analysis Method

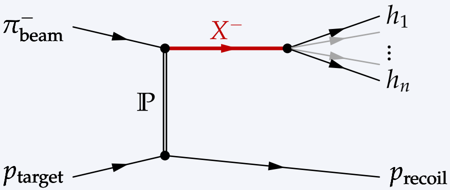

Two-stage analysis

$$\sigma(\tau; m_X) \propto \sum_{\epsilon=\pm 1} \left| \sum_i^{\text{waves}} T_i^\epsilon(m_X)\, A_i^\epsilon(\tau; m_X) \right|^2$$

1. **Determination of m_X dependence of spin-density matrix $\varrho_{ij}^\epsilon(m_X) = T_i^\epsilon(m_X)\, T_j^{\epsilon *}(m_X)$**
   - Independent maximum likelihood fits to τ distributions in narrow m_X bins
   - Take into account detection efficiency
   - No assumptions about resonance content of X
2. **Extraction of resonances**
   - χ^2 fit of resonance model to spin-density (sub)matrix

Outline

PWA of $\pi^- p \to \pi^- \eta^{(\prime)} p_{\text{recoil}}$

PLB **740** (2015) 303

- Odd-spin waves: spin-exotic quantum numbers
  - Disputed $J^{PC} = 1^{-+}$ resonance signals
    - $\pi_1(1400)$ in $\pi\eta$ and $\pi_1(1600)$ in $\pi\eta'$
- Comparison of $\pi\eta$ and $\pi\eta'$: information about flavor structure

Reconstruction from exclusive $\pi^-\pi^+\pi^-\gamma\gamma$ final state

- $\eta \to \pi^+\pi^-\pi^0$ with $\pi^0 \to \gamma\gamma$
- $\eta' \to \pi^+\pi^-\eta$ with $\eta \to \gamma\gamma$

PWA of $\pi^- p \to \pi^- \eta^{(\prime)} p_{\text{recoil}}$

- Odd-spin waves: spin-exotic quantum numbers
  - Disputed $J^{PC} = 1^{-+}$ resonance signals
    - $\pi_1(1400)$ in $\pi\eta$ and $\pi_1(1600)$ in $\pi\eta'$
- Comparison of $\pi\eta$ and $\pi\eta'$: information about flavor structure

Reconstruction from exclusive $\pi^-\pi^+\pi^-\gamma\gamma$ final state

- $\eta \to \pi^+\pi^-\pi^0$ with $\pi^0 \to \gamma\gamma$
- $\eta' \to \pi^+\pi^-\eta$ with $\eta \to \gamma\gamma$

$\pi^-\eta$ invariant mass

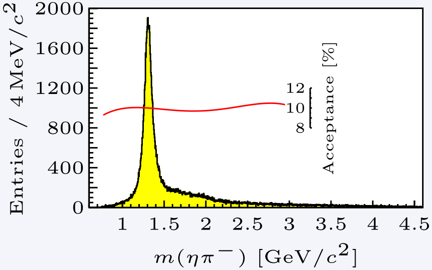

PWA of $\pi^- p \to \pi^- \eta^{(\prime)} p_{\text{recoil}}$

- Odd-spin waves: spin-exotic quantum numbers
  - Disputed $J^{PC} = 1^{-+}$ resonance signals
    - $\pi_1(1400)$ in $\pi\eta$ and $\pi_1(1600)$ in $\pi\eta'$
- Comparison of $\pi\eta$ and $\pi\eta'$: information about flavor structure

Reconstruction from exclusive $\pi^-\pi^+\pi^-\gamma\gamma$ final state

- $\eta \to \pi^+\pi^-\pi^0$ with $\pi^0 \to \gamma\gamma$
- $\eta' \to \pi^+\pi^-\eta$ with $\eta \to \gamma\gamma$

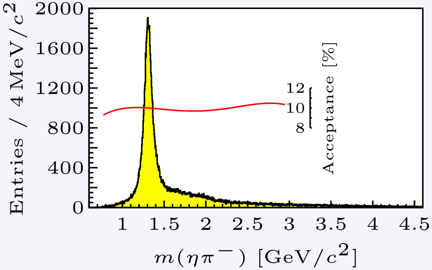

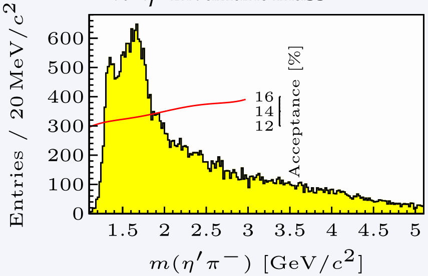

Comparison of $J^{PC} = 2^{++}$ Partial Waves

Quark-line picture for $n = (u, d)$ and pointlike resonances

- $\pi^- \eta$ and $\pi^- \eta'$ partial-wave intensities for spin J related by
  - Different phase space and barrier factors
  - Branching fraction ratio b of η and η' into $\pi^- \pi^+ \gamma\gamma$

$$N_J^{\pi\eta'}(m) \propto b \left[\frac{q^{\pi\eta'}(m)}{q^{\pi\eta}(m)} \right]^{2J+1} N_J^{\pi\eta}(m)$$

- q = breakup momentum

Comparison of $J^{PC} = 2^{++}$ Partial Waves

PLB **740** (2015) 303

Quark-line picture for $n = (u, d)$ and pointlike resonances

- $\pi^-\eta$ and $\pi^-\eta'$ partial-wave intensities for spin J related by
  - Different phase space and barrier factors
  - Branching fraction ratio b of η and η' into $\pi^-\pi^+\gamma\gamma$

$$N_J^{\pi\eta'}(m) \propto b \left[\frac{q^{\pi\eta'}(m)}{q^{\pi\eta}(m)}\right]^{2J+1} N_J^{\pi\eta}(m)$$

- q = breakup momentum

$\pi^-\eta$ final state

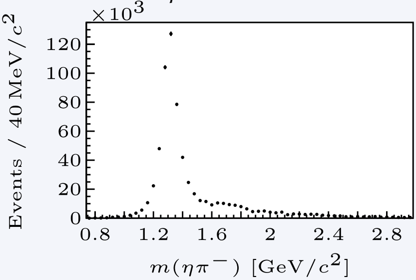

$\pi^-\eta'$ final state

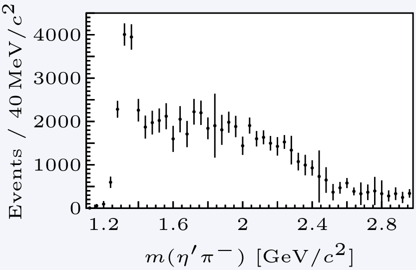

Comparison of $J^{PC} = 2^{++}$ Partial Waves

Quark-line picture for $n = (u,d)$ and pointlike resonances

- $\pi^-\eta$ and $\pi^-\eta'$ partial-wave intensities for spin J related by
  - Different phase space and barrier factors
  - Branching fraction ratio b of η and η' into $\pi^-\pi^+\gamma\gamma$

$$N_J^{\pi\eta'}(m) \propto b \left[\frac{q^{\pi\eta'}(m)}{q^{\pi\eta}(m)}\right]^{2J+1} N_J^{\pi\eta}(m)$$

- q = breakup momentum

$\pi^-\eta$ final state

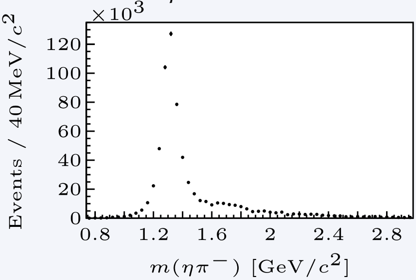

$\pi^-\eta'$ final state; $\pi^-\eta$ scaled

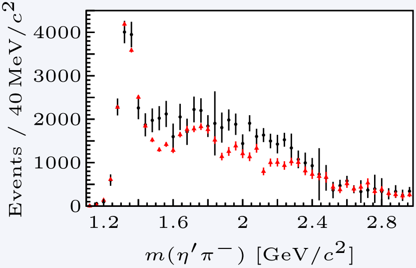

Even-Spin Waves

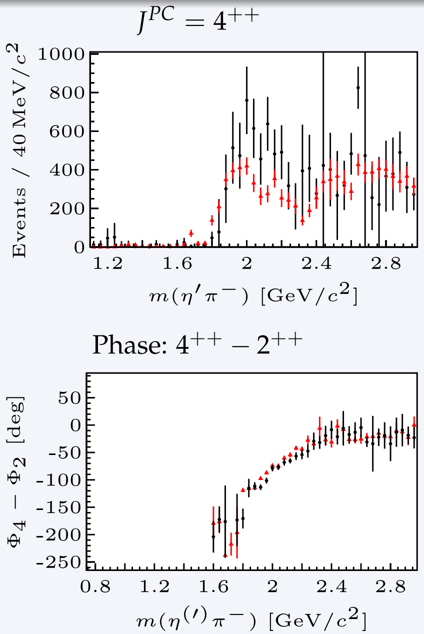

- Similar even-spin waves
- Intermediate states couple to same final-state flavour content
- Similar physical content also in nonresonant high-mass region

$\pi^-\eta'$ final state; $\pi^-\eta$ scaled

Even-Spin Waves

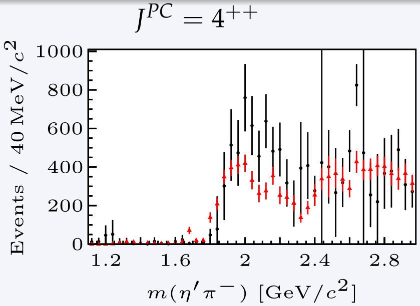

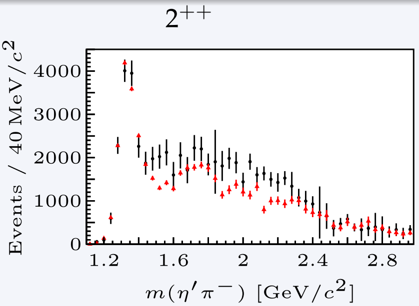

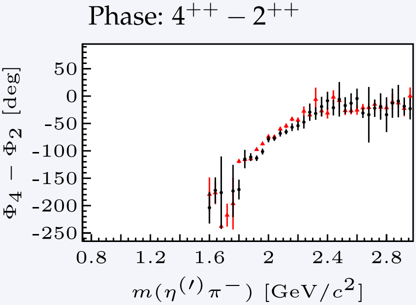

- Resonance-model fit (Breit-Wigner)
- $\frac{N(a_2 \to \pi\eta')}{N(a_2 \to \pi\eta)} = (5 \pm 2)\,\%$
- First-time measurement of $\frac{N(a_4 \to \pi\eta')}{N(a_4 \to \pi\eta)} = (23 \pm 7)\,\%$

$\pi^-\eta'$ final state; $\pi^-\eta$ scaled

$J^{PC} = 1^{-+}$ Spin-Exotic Wave

PLB **740** (2015) 303

Spin-exotic $J^{PC} = 1^{-+}$

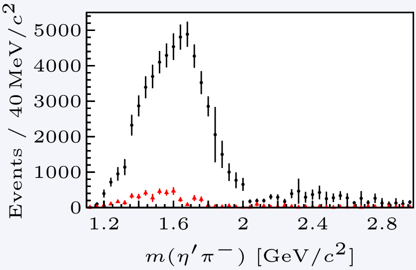

2^{++}

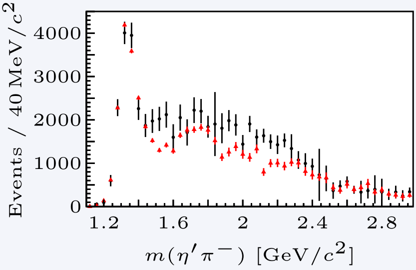

Phase: $1^{-+} - 2^{++}$

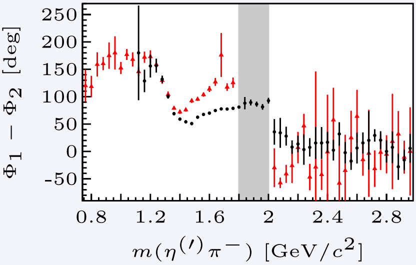

- 1^{-+} intensities very different
- Suppression in $\pi\eta$ channel predicted for intermediate $|q\bar{q}g\rangle$ state
- Different phase motion in 1.6 GeV/c^2 region

$\pi^-\eta'$ final state; $\pi^-\eta$ scaled

$J^{PC} = 1^{-+}$ Spin-Exotic Wave

PLB **740** (2015) 303

Spin-exotic $J^{PC} = 1^{-+}$

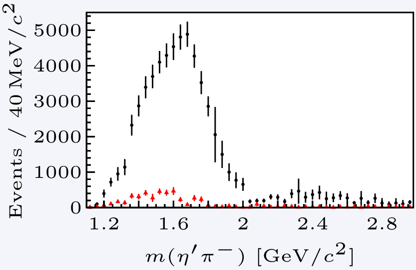

2^{++}

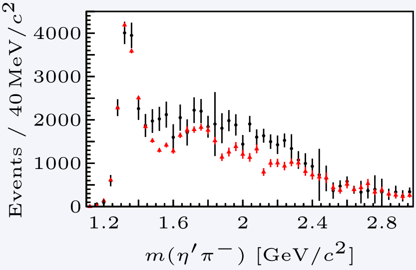

Phase: $1^{-+} - 2^{++}$

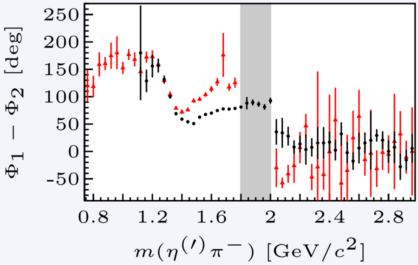

- 1^{-+} resonance interpretation requires better understanding of
  - 2^{++} wave
  - Nonresonant contributions

$\pi^-\eta'$ final state; $\pi^-\eta$ scaled

$J^{PC} = 1^{-+}$ Spin-Exotic Wave

Spin-exotic $J^{PC} = 1^{-+}$

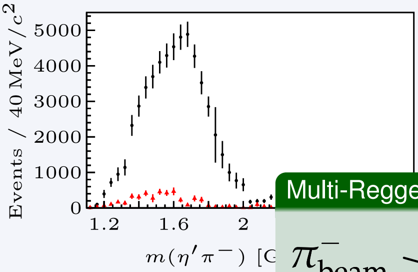

2^{++}

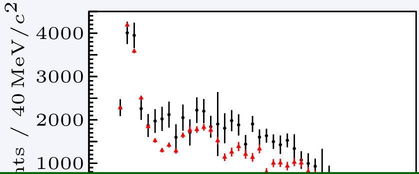

Phase: $1^{-+} - 2^{+}$

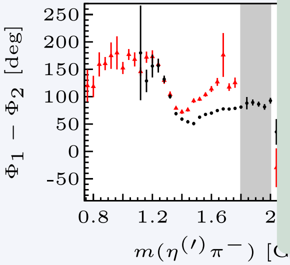

Multi-Regge exchange, e.g.

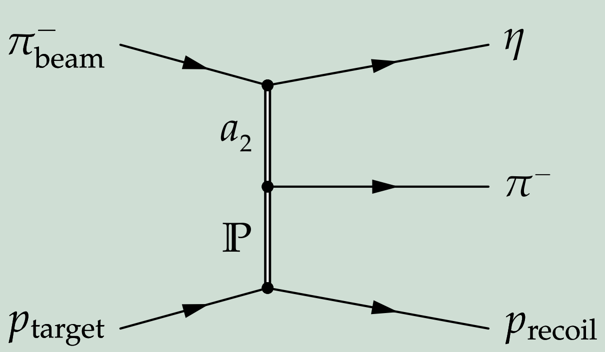

Outline

1. Introduction
   - Meson production in diffractive dissociation
   - Partial-wave analysis method
2. PWA of diffractively produced $\pi^-\eta$ and $\pi^-\eta'$ final states
   - Even partial waves similar
   - Exotic 1^{-+} much stronger in $\pi^-\eta'$
3. PWA of diffractively produced 3π final states
   - Observation of a new narrow axial-vector meson $a_1(1420)$
   - $J^{PC} = 1^{-+}$ spin-exotic partial wave
4. Conclusions and outlook

Partial-Wave Analysis: $\pi^-\pi^+\pi^-$ Final State

[arXiv:1509.00992]

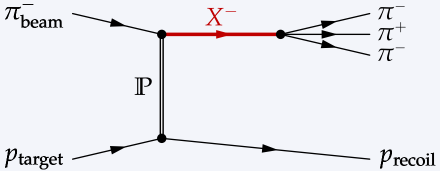

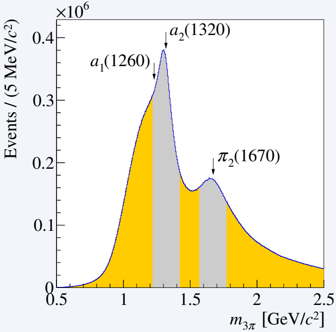

Strong $\pi^+\pi^-$ correlations in $X^- \to \pi^-\pi^+\pi^-$ decay

Partial-Wave Analysis: $\pi^-\pi^+\pi^-$ Final State

[arXiv:1509.00992]

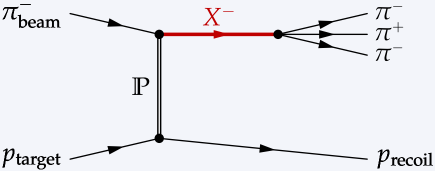

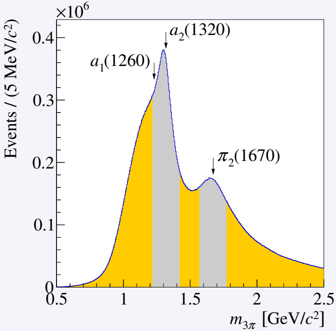

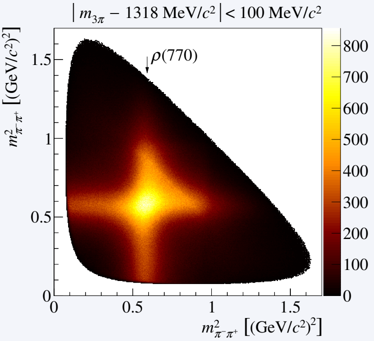

Strong $\pi^+\pi^-$ correlations in $X^- \to \pi^-\pi^+\pi^-$ decay

Partial-Wave Analysis: $\pi^-\pi^+\pi^-$ Final State

[arXiv:1509.00992]

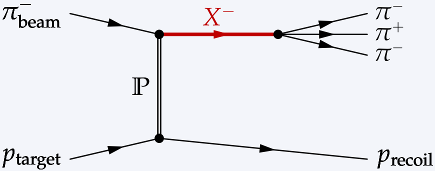

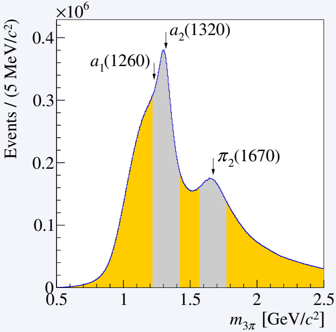

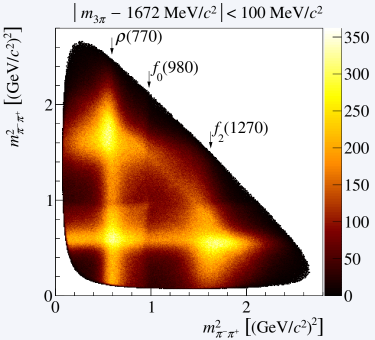

Strong $\pi^+\pi^-$ correlations in $X^- \to \pi^-\pi^+\pi^-$ decay

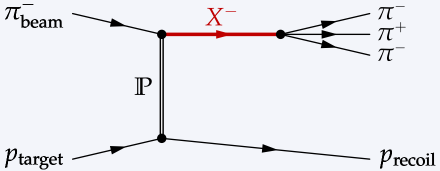

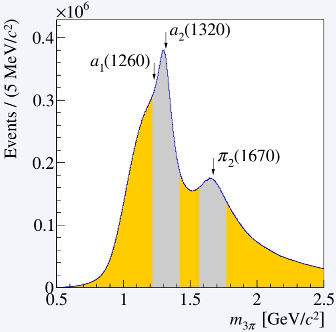

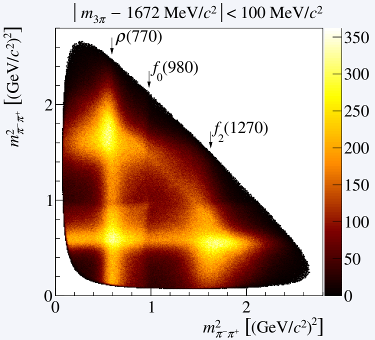

Strong $\pi^+\pi^-$ correlations in $X^- \to \pi^-\pi^+\pi^-$ decay

Partial-Wave Analysis: $\pi^-\pi^+\pi^-$ Final State

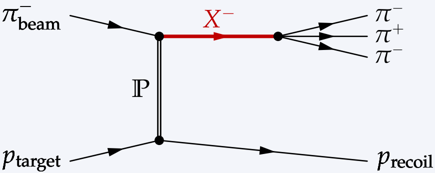

Isobar model

- X^- decays via intermediate $\pi^+\pi^-$ resonance = *"isobar"*
  - $[\pi\pi]_S$ — $J^{PC} = 0^{++}$
  - $\rho(770)$ — 1^{--}
  - $f_0(980)$ — 0^{++}
  - $f_2(1270)$ — 2^{++}
  - $f_0(1500)$ — 0^{++}
  - $\rho_3(1690)$ — 3^{--}
- PWA requires precise knowledge of isobar $\rightarrow \pi^+\pi^-$ amplitude

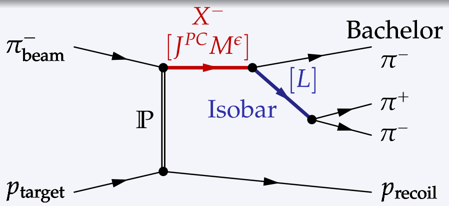

Isobar model

- X^- decays via intermediate $\pi^+\pi^-$ resonance = *"isobar"*
  - $[\pi\pi]_S$ $J^{PC} = 0^{++}$
  - $\rho(770)$ 1^{--}
  - $f_0(980)$ 0^{++}
  - $f_2(1270)$ 2^{++}
  - $f_0(1500)$ 0^{++}
  - $\rho_3(1690)$ 3^{--}
- PWA requires precise knowledge of isobar $\rightarrow \pi^+\pi^-$ amplitude

Partial-Wave Analysis: $\pi^-\pi^+\pi^-$ Final State

[arXiv:1509.00992]

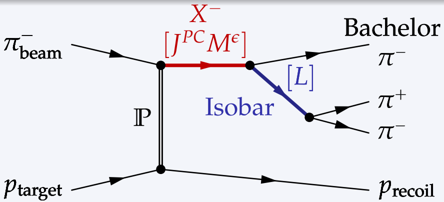

Isobar model

- X^- decays via intermediate $\pi^+\pi^-$ resonance = *"isobar"*
  - $[\pi\pi]_S$ $J^{PC} = 0^{++}$
  - $\rho(770)$ 1^{--}
  - $f_0(980)$ 0^{++}
  - $f_2(1270)$ 2^{++}
  - $f_0(1500)$ 0^{++}
  - $\rho_3(1690)$ 3^{--}
- PWA requires precise knowledge of isobar $\rightarrow \pi^+\pi^-$ amplitude

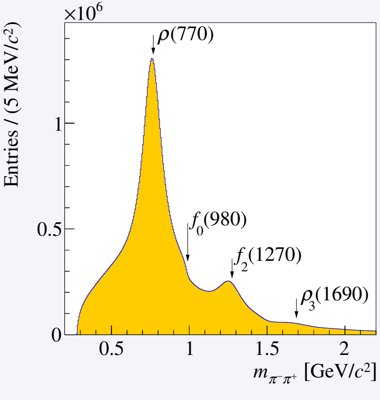

PWA of $\pi^- p \to (3\pi)^- p_{\text{recoil}}$

Two Data Sets

1. $\pi^-\pi^+\pi^-$ (50 M events)
2. Crosscheck with $\pi^-\pi^0\pi^0$ (3.5 M events)
   - Very different acceptance
   - Isobars separated by isospin
     - $I = 1$ isobars: $\pi^-\pi^0$
     - $I = 0$ isobars: $\pi^0\pi^0$

Complex correlation of $m_{3\pi}$ and t'

- Two-dimensional PWA in bins of t' and $m_{3\pi}$
  - $\pi^-\pi^+\pi^-$: 11 t' bins
  - $\pi^-\pi^0\pi^0$: 8 t' bins
- Better disentanglement of resonant and nonresonant contributions

PWA of $\pi^- p \to (3\pi)^- p_{\text{recoil}}$

Two Data Sets

1. $\pi^-\pi^+\pi^-$ (50 M events)
2. Crosscheck with $\pi^-\pi^0\pi^0$ (3.5 M events)
   - Very different acceptance
   - Isobars separated by isospin
     - $I = 1$ isobars: $\pi^-\pi^0$
     - $I = 0$ isobars: $\pi^0\pi^0$

Complex correlation of $m_{3\pi}$ and t'

- Two-dimensional PWA in bins of t' **and** $m_{3\pi}$
  - $\pi^-\pi^+\pi^-$: 11 t' bins
  - $\pi^-\pi^0\pi^0$: 8 t' bins
- Better disentanglement of resonant and nonresonant contributions

$800 < m_{3\pi} < 850$ MeV$/c^2$

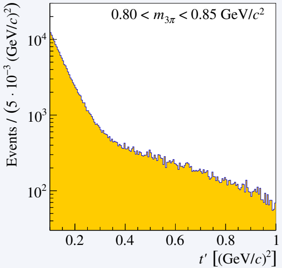

$1600 < m_{3\pi} < 1650$ MeV$/c^2$

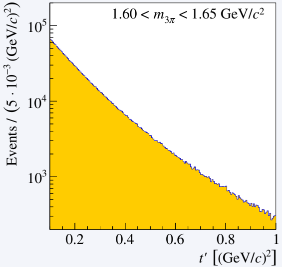

PWA of $\pi^- p \to (3\pi)^- p_{\text{recoil}}$

Two Data Sets

1. $\pi^-\pi^+\pi^-$ (50 M events)
2. Crosscheck with $\pi^-\pi^0\pi^0$ (3.5 M events)
   - Very different acceptance
   - Isobars separated by isospin
     - $I = 1$ isobars: $\pi^-\pi^0$
     - $I = 0$ isobars: $\pi^0\pi^0$

Complex correlation of $m_{3\pi}$ and t'

- Two-dimensional PWA in bins of t' and $m_{3\pi}$
  - $\pi^-\pi^+\pi^-$: 11 t' bins
  - $\pi^-\pi^0\pi^0$: 8 t' bins
- Better disentanglement of resonant and nonresonant contributions

$0.10 < t' < 0.12\ (\text{GeV}/c)^2$

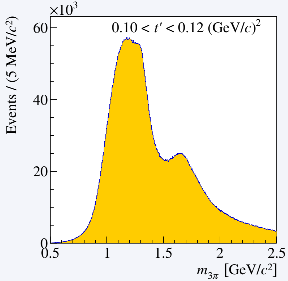

$0.44 < t' < 1.00\ (\text{GeV}/c)^2$

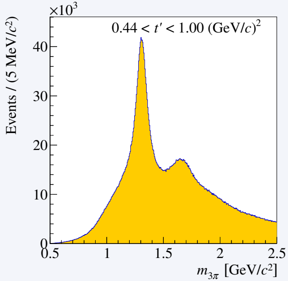

PWA of $\pi^- p \to \pi^-\pi^+\pi^- p_{\text{recoil}}$: Major Waves

[arXiv:1509.00992]

- $\pi^-\pi^+\pi^-$ invariant mass spectrum
- $1^{++}0^+ \rho(770)\pi S$: $a_1(1260)$
- $2^{++}1^+ \rho(770)\pi D$: $a_2(1320)$
- $2^{-+}0^+ f_2(1270)\pi S$: $\pi_2(1670)$

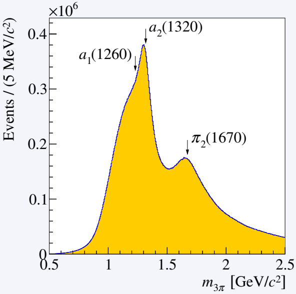

PWA of $\pi^- p \to \pi^-\pi^+\pi^- p_{\text{recoil}}$: Major Waves [arXiv:1509.00992]

- $\pi^-\pi^+\pi^-$ invariant mass spectrum
- $1^{++}0^+\rho(770)\pi S$: $a_1(1260)$
- $2^{++}1^+\rho(770)\pi D$: $a_2(1320)$
- $2^{-+}0^+ f_2(1270)\pi S$: $\pi_2(1670)$

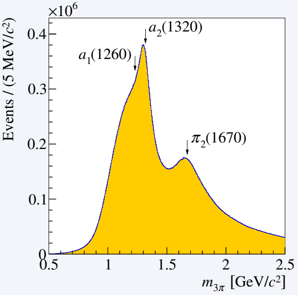

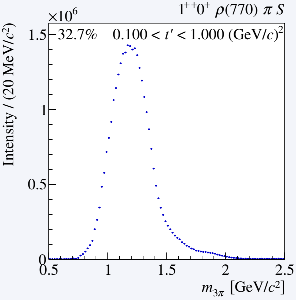

PWA of $\pi^- p \to \pi^-\pi^+\pi^- p_{\text{recoil}}$: Major Waves

[arXiv:1509.00992]

- $\pi^-\pi^+\pi^-$ invariant mass spectrum
- $1^{++}\,0^+\,\rho(770)\pi S$: $a_1(1260)$
- $2^{++}\,1^+\,\rho(770)\pi D$: $a_2(1320)$
- $2^{-+}\,0^+\,f_2(1270)\pi S$: $\pi_2(1670)$

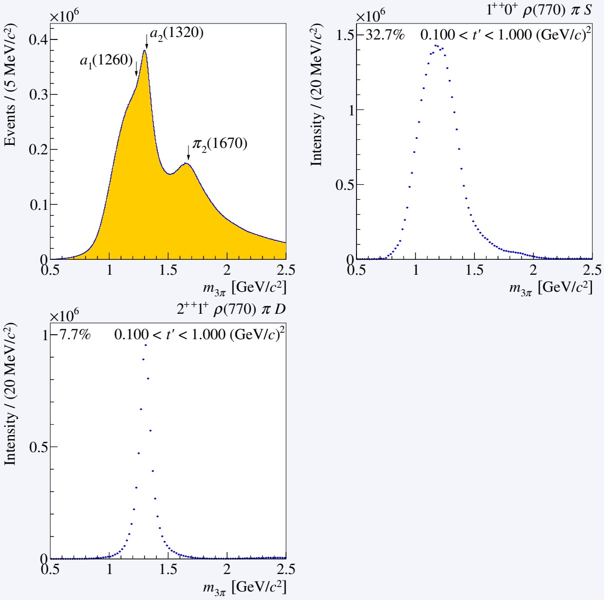

PWA of $\pi^- p \to \pi^-\pi^+\pi^- p_{\text{recoil}}$: Major Waves [arXiv:1509.00992]

- $\pi^-\pi^+\pi^-$ invariant mass spectrum
- $1^{++}0^+ \rho(770)\pi S$: $a_1(1260)$
- $2^{++}1^+ \rho(770)\pi D$: $a_2(1320)$
- $2^{-+}0^+ f_2(1270)\pi S$: $\pi_2(1670)$

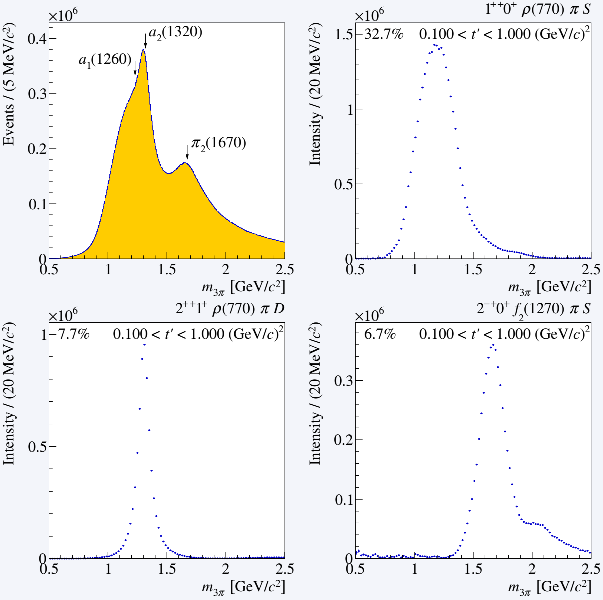

PWA of $\pi^- p \to \pi^-\pi^+\pi^- p_{\text{recoil}}$: Major Waves

- $\pi^-\pi^+\pi^-$ invariant mass spectrum
- $1^{++}\,0^+\,\rho(770)\pi S$: $a_1(1260)$
- $2^{++}\,1^+\,\rho(770)\pi D$: $a_2(1320)$
- $2^{-+}\,0^+\,f_2(1270)\pi S$: $\pi_2(1670)$

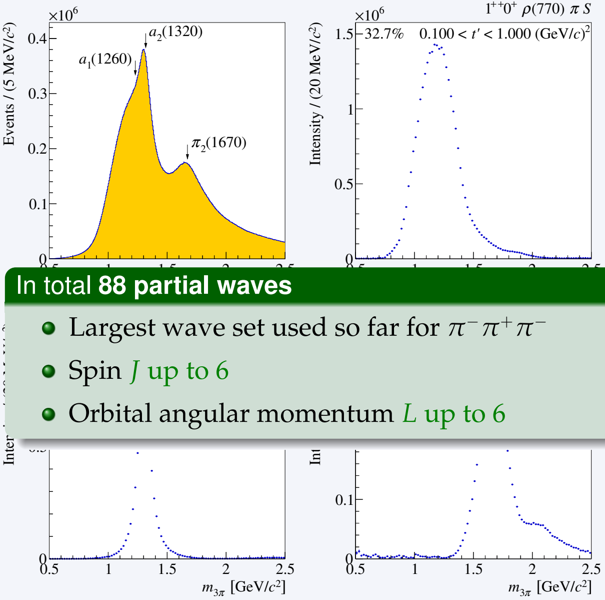

In total 88 partial waves

- Largest wave set used so far for $\pi^-\pi^+\pi^-$
- Spin J up to 6
- Orbital angular momentum L up to 6

PWA of $\pi^- p \to \pi^-\pi^+\pi^- p_{\text{recoil}}$: Selected Small Waves

[arXiv:1509.00992]

$4^{++}\,1^+\,\rho(770)\pi G$

- $a_4(2040)$

$0^{-+}\,0^+\,f_0(980)\pi S$

- $\pi(1800)$

$1^{++}\,0^+\,f_0(980)\pi P$

- **Unexpected peak around 1.4 GeV/c^2**
- Small intensity: $\approx 0.3\%$
- Similar signal in $\pi^-\pi^0\pi^0$

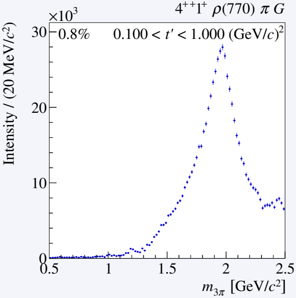

PWA of $\pi^- p \to \pi^-\pi^+\pi^- p_{\text{recoil}}$: Selected Small Waves

[arXiv:1509.00992]

$4^{++}\,1^+\,\rho(770)\pi G$

- $a_4(2040)$

$0^{-+}\,0^+\,f_0(980)\pi S$

- $\pi(1800)$

$1^{++}\,0^+\,f_0(980)\pi P$

- **Unexpected peak around 1.4 GeV/c^2**
- Small intensity: $\approx 0.3\%$
- Similar signal in $\pi^-\pi^0\pi^0$

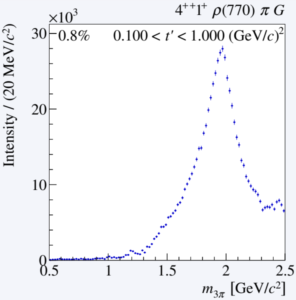

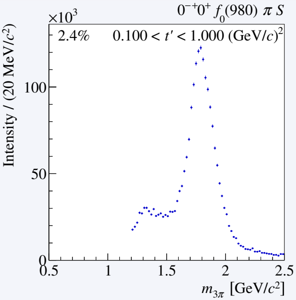

PWA of $\pi^- p \to \pi^- \pi^+ \pi^- p_{\text{recoil}}$: Selected Small Waves

[arXiv:1509.00992]

$4^{++} 1^+ \rho(770) \pi G$

- $a_4(2040)$

$0^{-+} 0^+ f_0(980) \pi S$

- $\pi(1800)$

$1^{++} 0^+ f_0(980) \pi P$

- **Unexpected peak around 1.4 GeV/c^2**
- Small intensity: $\approx 0.3\%$
- Similar signal in $\pi^- \pi^0 \pi^0$

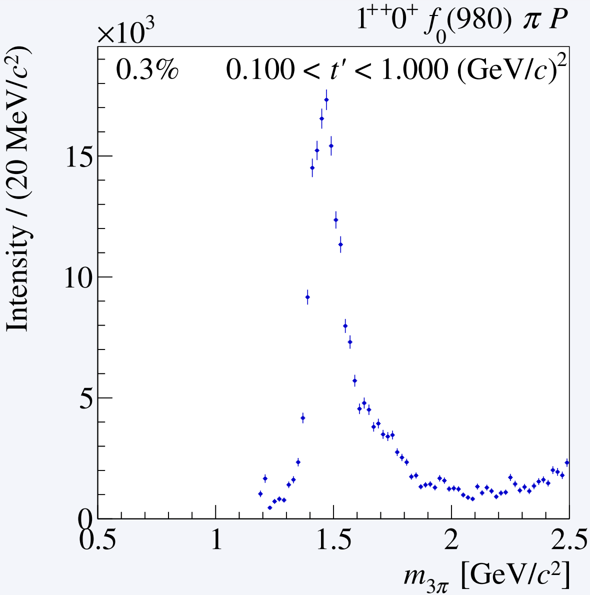

PWA of $\pi^- p \to \pi^-\pi^+\pi^- p_{\text{recoil}}$: Selected Small Waves

$4^{++}\, 1^+\, \rho(770)\pi G$

- $a_4(2040)$

$0^{-+}\, 0^+\, f_0(980)\pi S$

- $\pi(1800)$

$1^{++}\, 0^+\, f_0(980)\pi P$

- **Unexpected peak around 1.4 GeV/c^2**
- Small intensity: $\approx 0.3\%$
- Similar signal in $\pi^-\pi^0\pi^0$

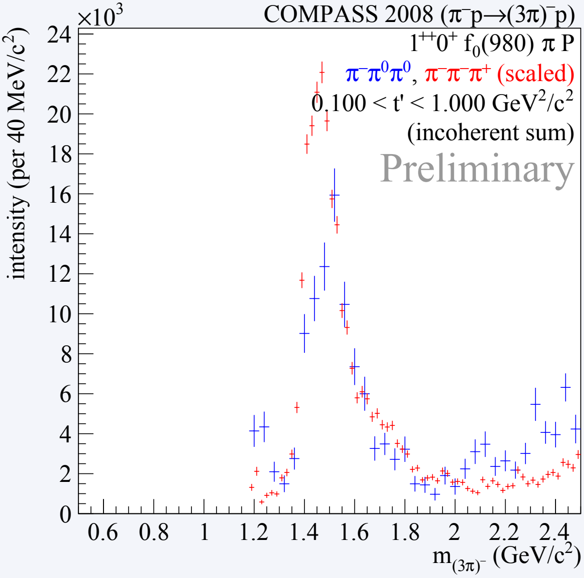

$\pi^-\pi^0\pi^0$

$\pi^-\pi^+\pi^-$ scaled for each plot

Is Peak in $1^{++}\,0^{+}\,f_0(980)\,\pi P$ Wave a Model Artifact?

Novel analysis method

(inspired by E791 analysis, PRD **73** (2006) 032204)

- Replace $J^{PC} = 0^{++}$ isobar parametrizations by piece-wise constant amplitudes in $m_{\pi^+\pi^-}$ bins
- Extract $m_{3\pi}$ dependence of 0^{++} isobar amplitude from data
  - Drastic reduction of model bias
  - *Caveat:* significant increase in number of fit parameters
- Result: the $a_1(1420)$ signal is indep. on the $f_0(980)$ description

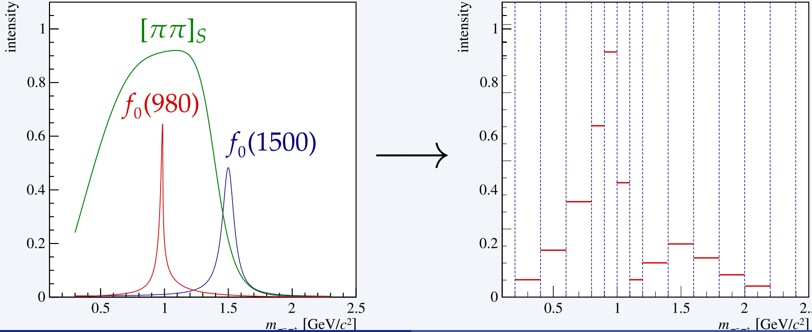

Is Peak in $1^{++}\,0^{+}\,f_0(980)\,\pi P$ Wave a Model Artifact?

Novel analysis method
(inspired by E791 analysis, PRD **73** (2006) 032204)

- Replace $J^{PC} = 0^{++}$ isobar parametrizations by piece-wise constant amplitudes in $m_{\pi^+\pi^-}$ bins
- Extract $m_{3\pi}$ dependence of 0^{++} isobar amplitude from data
  - Drastic reduction of model bias
  - *Caveat:* significant increase in number of fit parameters
- Result: the $a_1(1420)$ signal is indep. on the $f_0(980)$ description

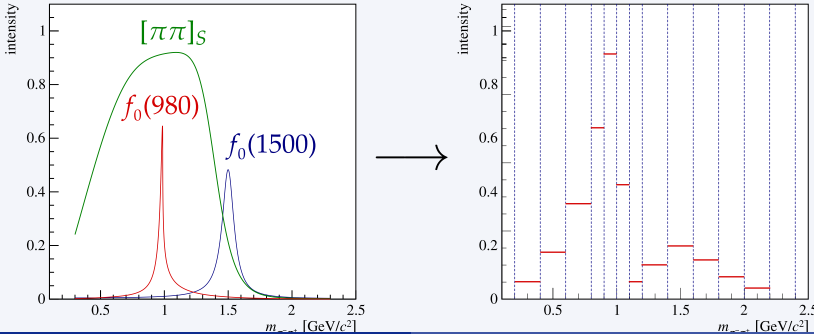

Is Peak in $1^{++}\,0^{+}\,f_0(980)\,\pi P$ Wave a Model Artifact?

Novel analysis method

(inspired by E791 analysis, PRD **73** (2006) 032204)

- Replace $J^{PC} = 0^{++}$ isobar parametrizations by piece-wise constant amplitudes in $m_{\pi^+\pi^-}$ bins
- Extract $m_{3\pi}$ dependence of 0^{++} isobar amplitude from data
  - Drastic reduction of model bias
  - *Caveat:* significant increase in number of fit parameters
- Result: the $a_1(1420)$ signal is indep. on the $f_0(980)$ description

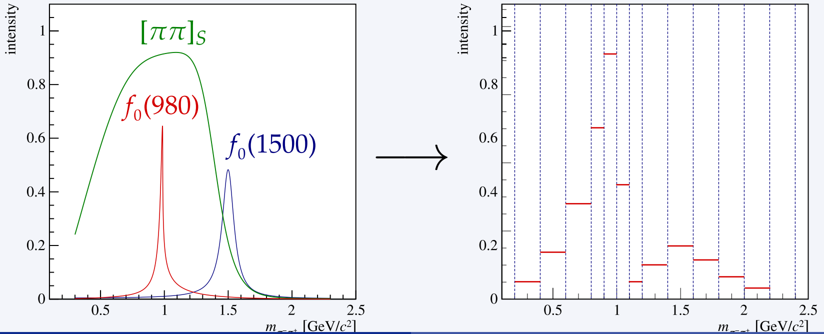

PRL **115** (2015) 082001

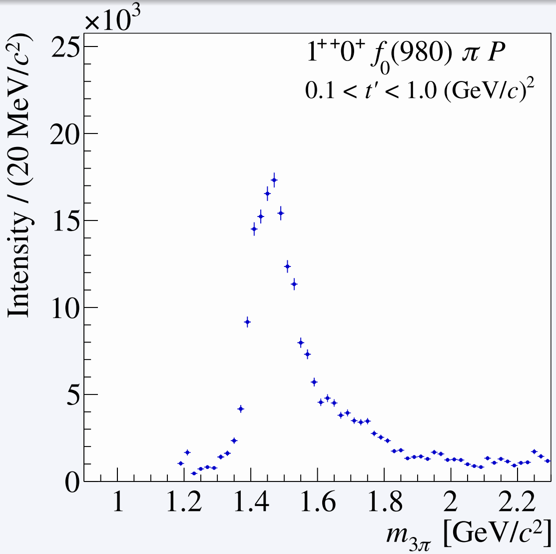

- Coherent sum of resonant (Breit-Wigner) and nonresonant terms

Resonance-Model Fit

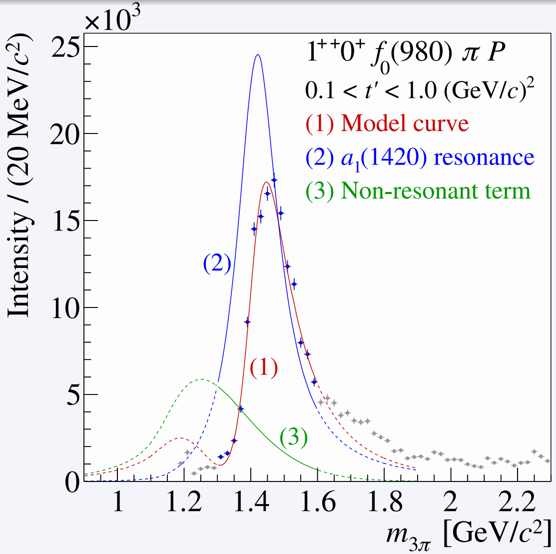

- Coherent sum of resonant (Breit-Wigner) and nonresonant terms

Resonance-Model Fit

PRL **115** (2015) 082001

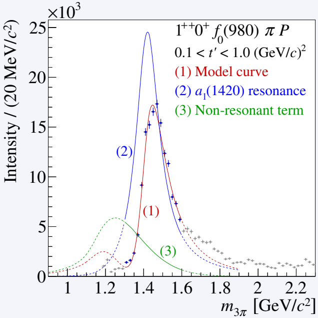

- 1^{++} peak consistent with Breit-Wigner resonance
- $a_1(1420)$:
  $M_0 = 1414^{+15}_{-13}$ MeV/c^2 $\Gamma_0 = 153^{+8}_{-23}$ MeV/c^2

Resonance-Model Fit

PRL **115** (2015) 082001

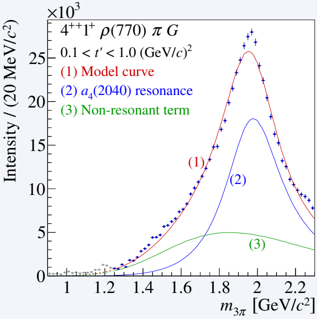

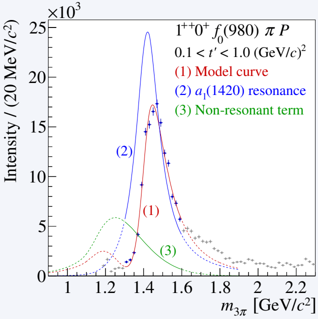

- 1^{++} peak consistent with Breit-Wigner resonance
- $a_1(1420)$: $M_0 = 1414^{+15}_{-13}\,\text{MeV}/c^2$ $\Gamma_0 = 153^{+8}_{-23}\,\text{MeV}/c^2$

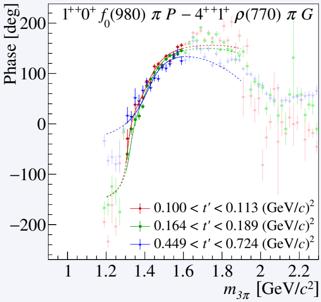

Resonance-Model Fit

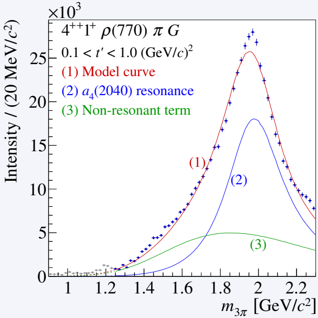

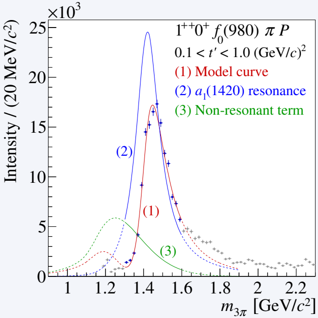

- 1^{++} peak consistent with Breit-Wigner resonance
- $a_1(1420)$:
  $M_0 = 1414^{+15}_{-13}\,\mathrm{MeV}/c^2\,\Gamma_0 = 153^{+8}_{-23}\,\mathrm{MeV}/c^2$

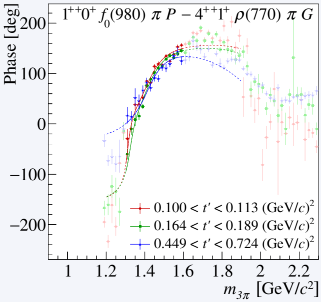

$a_1(1420)$

Nature unclear

- No quark-model states expected at $1.4\,\mathrm{GeV}/c^2$
- Ground state $a_1(1260)$ very close and wider
- Seen only in $f_0(980)\pi$ decay mode
- Isospin partner of narrow $f_1(1420)$?
- Suspiciously close to $K\bar{K}^*$ threshold

$a_1(1420)$

PRL **115** (2015) 082001

Several proposed explanations

- Two-quark-tetraquark mixed state [Wang, arXiv:1401.1134]
- Tetraquark with mixed flavor symmetry

  [Chen *et al.*, PRD **91** (2015) 094022]
- Two-channel unitarized Deck amplitude + direct $a_1(1260)$ production

  [Basdevant and Berger, PRL **114** (2015) 192001 and arXiv:1501.04643]
- Singularity (branching point) in triangle diagram

  [Mikhasenko *et al.*, PRD **91** (2015) 094015]

$a_1(1420)$

Several proposed explanations

- Two-quark-tetraquark mixed state [Wang, arXiv:1401.1134]
- Tetraquark with mixed flavor symmetry
  [Chen *et al.*, PRD **91** (2015) 094022]
- Two-channel unitarized Deck amplitude + direct $a_1(1260)$ production
  [Basdevant and Berger, PRL **114** (2015) 192001 and arXiv:1501.04643]
- Singularity (branching point) in triangle diagram
  [Mikhasenko *et al.*, PRD **91** (2015) 094015]

$a_1(1420)$

Several proposed explanations

- Two-quark-tetraquark mixed state [Wang, arXiv:1401.1134]
- Tetraquark with mixed flavor symmetry
  [Chen *et al.*, PRD **91** (2015) 094022]
- Two-channel unitarized Deck amplitude + direct $a_1(1260)$ production
  [Basdevant and Berger, PRL **114** (2015) 192001 and arXiv:1501.04643]
- Singularity (branching point) in triangle diagram
  [Mikhasenko *et al.*, PRD **91** (2015) 094015]

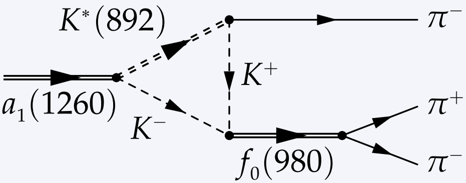

Spin-Exotic $J^{PC} = 1^{-+}$ Signal in $(3\pi)^-$ PWA

- Broad intensity bump
- Similar in both channels

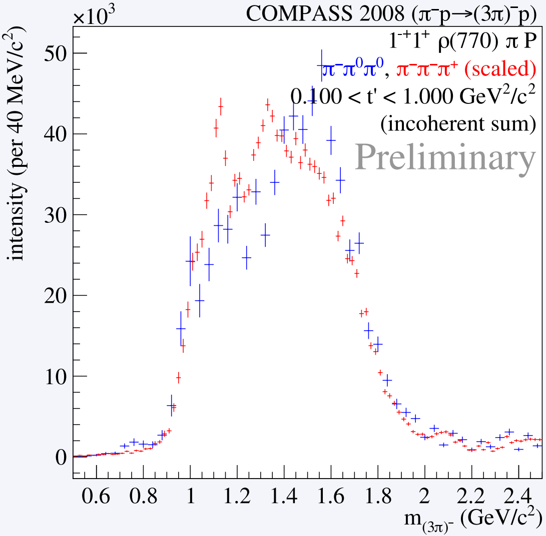

$\pi^-\pi^0\pi^0$

$\pi^-\pi^+\pi^-$ scaled

Spin-Exotic $J^{PC} = 1^{-+}$ Signal in $\pi^-\pi^+\pi^-$ PWA

Drastic Change of Mass Spectrum with t'

"Low" $t' \approx 0.1\ (\text{GeV}/c)^2$

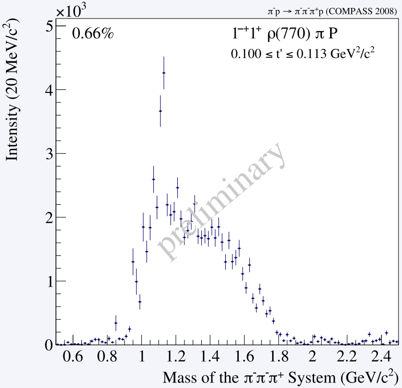

"High" $t' \approx 0.8\ (\text{GeV}/c)^2$

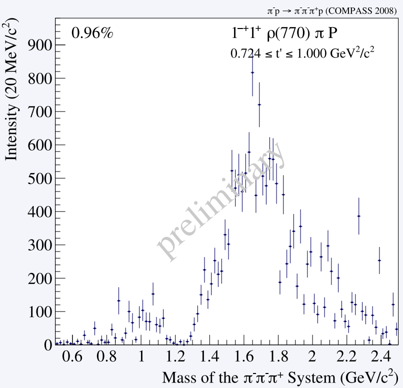

- Dominant nonresonant contribution
  - Needs to be better understood in order to extract resonance content

Deck effect

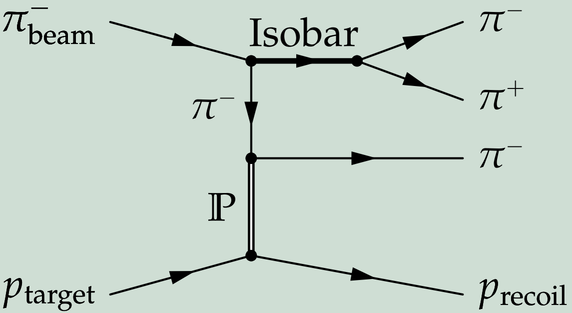

- MC pseudodata generated according to model of Deck amplitude

  based on ACCMOR, NPB **182** (1981) 269

- Analyzed like real data

Spin-Exotic $J^{PC} = 1^{-+}$ Signal in $\pi^-\pi^+\pi^-$ PWA

Deck-Model for Nonresonant Component

"Low" $t' \approx 0.1\ (\mathrm{GeV}/c)^2$

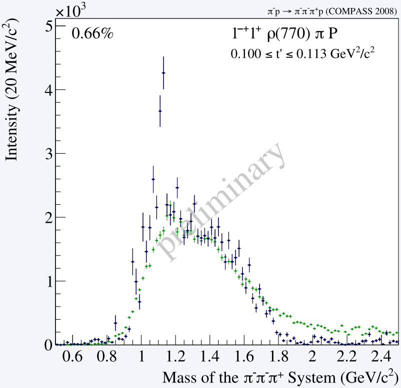

"High" $t' \approx 0.8\ (\mathrm{GeV}/c)^2$

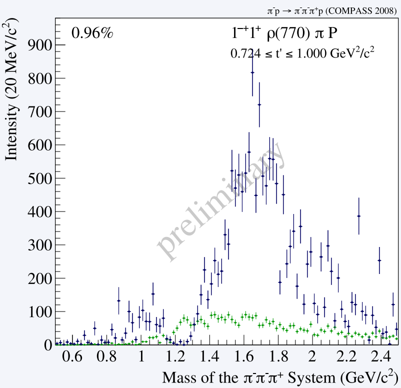

- Deck MC scaled to t'-summed intensity
  - Similar mass spectrum at low t'
  - Different shape at high t'

Spin-Exotic $J^{PC} = 1^{-+}$ Signal in $\pi^-\pi^+\pi^-$ PWA

Relative Phase w.r.t. $1^{++}\,0^+\,\rho(770)\pi S$ Wave

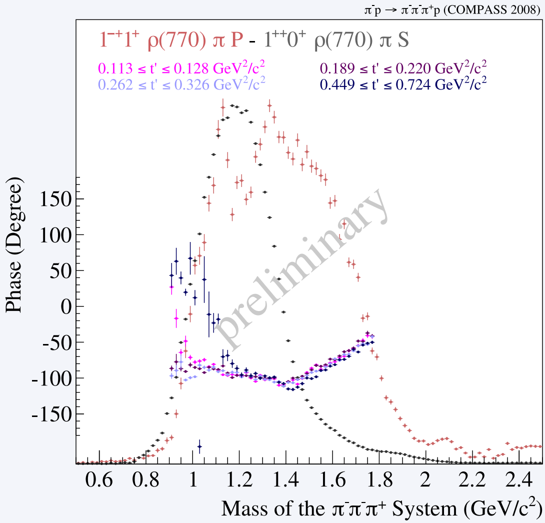

- Slow phase 60° motion in 1.6 GeV/c^2 region independent of t'

Outline

Conclusions and Outlook

Precise data on pion diffraction

- PWA reliably extracts even very small signals
  - New axial-vector state $a_1(1420)$ in $(3\pi)^-$ final states
- Novel analysis schemes:
  - PWA in bins of t'
    - Better separation of resonant and nonresonant contribution
  - Extraction of $\pi\pi$ S-wave amplitude from $\pi^-\pi^+\pi^-$ system
    - Study dependence on 3π source
    - Study rescattering effects
    - Extension to higher $\pi\pi$ waves

Conclusions and Outlook

Nonresonant contributions play important role

- Limit extraction of resonance parameters
- First studies using Deck models
- Extraction of nonresonant contributions from data
  - Collaboration with JPAC: Veneziano amplitudes + finite-energy sum rules

Other ongoing analyses

- Pion diffraction into $\pi^-\eta\eta$, $\pi^-\pi^0\omega$, $K\bar{K}\pi$, $K\bar{K}\pi\pi$, ...
- Kaon diffraction into $K^-\pi^+\pi^-$
- Central-production reactions
- $\pi\gamma$ scattering using Primakoff reactions on heavy targets

Conclusions and Outlook

Nonresonant contributions play important role

- Limit extraction of resonance parameters
- First studies using Deck models
- Extraction of nonresonant contributions from data
  - Collaboration with JPAC: Veneziano amplitudes + finite-energy sum rules

Other ongoing analyses

- Pion diffraction into $\pi^- \eta \eta$, $\pi^- \pi^0 \omega$, $K\bar{K}\pi$, $K\bar{K}\pi\pi$, ...
- Kaon diffraction into $K^- \pi^+ \pi^-$
- Central-production reactions
- $\pi\gamma$ scattering using Primakoff reactions on heavy targets

Outline

Meson Production in Diffractive Dissociation

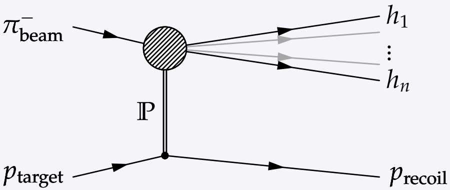

- Soft scattering of beam particle off target
  - Production of n forward-going hadrons
  - Target particle stays intact
- At 190 GeV/c, interaction dominated by space-like pomeron exchange
- All final-state particles are measured

Meson Production in Diffractive Dissociation

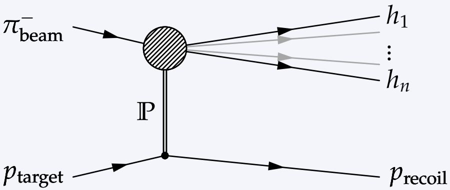

- Exclusive measurement
  - Clean data sample
- Reduced four-momentum transfer squared $t' \equiv |t| - |t|_{\text{min}}$
  - Analyzed range: $0.1 < t' < 1.0\,(\text{GeV}/c)^2$

Example: $\pi^-\pi^+\pi^-$ final state

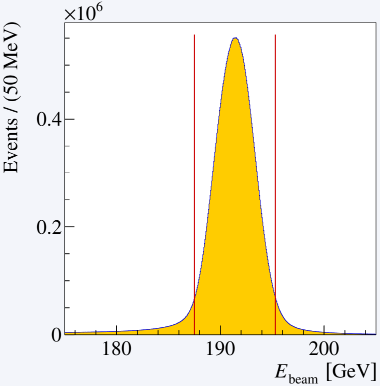

Meson Production in Diffractive Dissociation

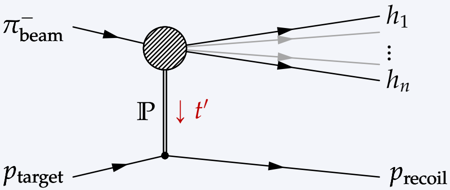

- Exclusive measurement
  - Clean data sample
- Reduced four-momentum transfer squared $t' \equiv |t| - |t|_{\text{min}}$
  - Analyzed range: $0.1 < t' < 1.0\,(\text{GeV}/c)^2$

Example: $\pi^-\pi^+\pi^-$ final state

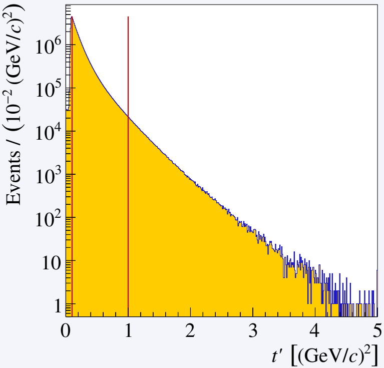

Partial-Wave Analysis Method

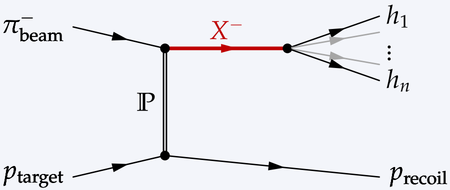

Ansatz: **Factorization of production and decay**

$$\sigma(\tau; m_X) \propto \sum_{\epsilon=\pm1} \left| \sum_i^{\mathrm{waves}} T_i^\epsilon(m_X)\, A_i^\epsilon(\tau; m_X) \right|^2$$

- Transition amplitudes $T_i^\epsilon(m_X)$ contain interesting physics
- Decay amplitudes $A_i^\epsilon(\tau; m_X)$
  - Describe kinematic τ distribution of partial waves
  - Calculable using isobar model (for $n > 2$) and helicity formalism (Wigner D-functions)
- $\epsilon = \pm1$: naturalities of exchange particle
  - 190 GeV/c beam momentum $\Longrightarrow$ pomeron ($\epsilon = +1$) dominates

Partial-Wave Analysis Method

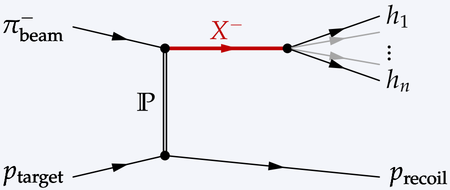

Ansatz: Factorization of production and decay

$$\sigma(\tau; m_X) \propto \sum_{\epsilon=\pm 1} \left| \sum_i^{\text{waves}} T_i^\epsilon(m_X)\, A_i^\epsilon(\tau; m_X) \right|^2$$

- Transition amplitudes $T_i^\epsilon(m_X)$ contain interesting physics
- Decay amplitudes $A_i^\epsilon(\tau; m_X)$
  - Describe kinematic τ distribution of partial waves
  - Calculable using isobar model (for $n > 2$) and helicity formalism (Wigner D-functions)
- $\epsilon = \pm 1$: naturalities of exchange particle
  - 190 GeV/c beam momentum $\Longrightarrow$ pomeron ($\epsilon = +1$) dominates

Partial-Wave Analysis Method

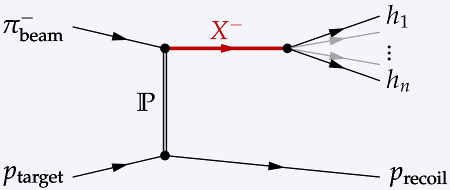

Ansatz: Factorization of production and decay

$$\sigma(\tau; m_X) \propto \sum_{\epsilon=\pm1} \left| \sum_i^{\text{waves}} T_i^\epsilon(m_X)\, A_i^\epsilon(\tau; m_X) \right|^2$$

- Transition amplitudes $T_i^\epsilon(m_X)$ contain interesting physics
- Decay amplitudes $A_i^\epsilon(\tau; m_X)$
  - Describe kinematic τ distribution of partial waves
  - Calculable using isobar model (for $n > 2$) and helicity formalism (Wigner D-functions)
- $\epsilon = \pm1$: naturalities of exchange particle
  - 190 GeV/c beam momentum $\Longrightarrow$ pomeron ($\epsilon = +1$) dominates

$\pi\pi$ S-Wave Amplitude in $J^{PC} = 1^{++}$ 3π Wave [arXiv:1509.00992]

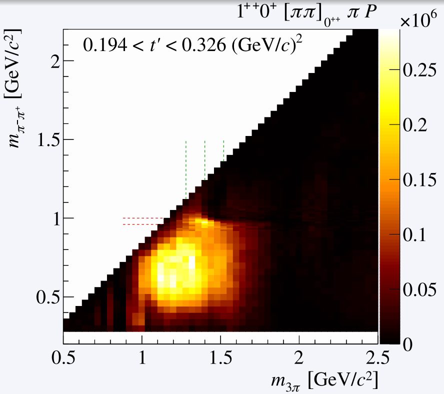

- Correlation of 3π intensity around 1.4 GeV/c^2 with $f_0(980)$
- $f_0(980)$ semicircle in Argand diagram
- Confirms that $f_0(980)\pi$ signal is *not* an artifact of isobar parametrization

$\pi\pi$ S-Wave Amplitude in $J^{PC} = 1^{++}$ 3π Wave [arXiv:1509.00992]

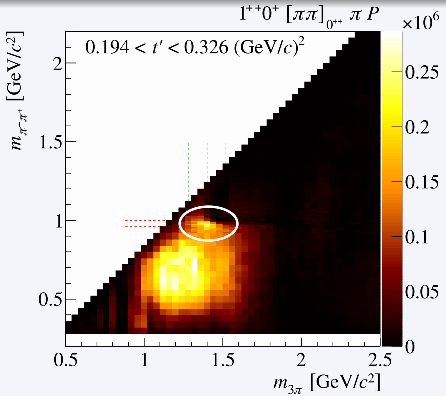

- Correlation of 3π intensity around $1.4\,\mathrm{GeV}/c^2$ with $f_0(980)$
- $f_0(980)$ semicircle in Argand diagram
- Confirms that $f_0(980)\pi$ signal is *not* an artifact of isobar parametrization

$\pi\pi$ S-Wave Amplitude in $J^{PC} = 1^{++}$ 3π Wave [arXiv:1509.00992]

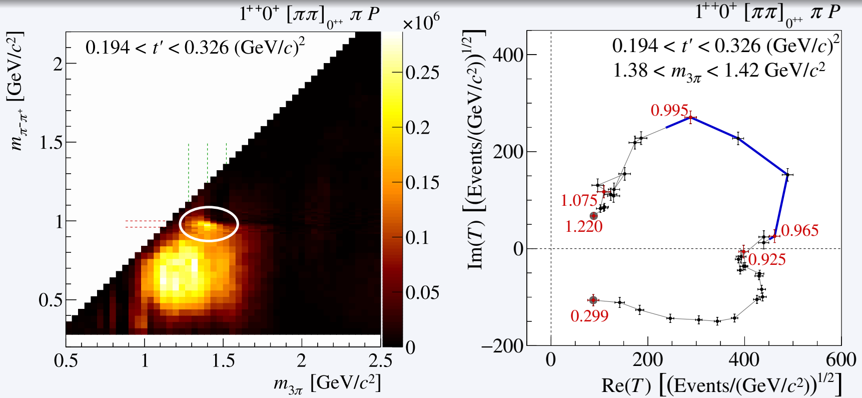

- Correlation of 3π intensity around $1.4\,\text{GeV}/c^2$ with $f_0(980)$
- $f_0(980)$ semicircle in Argand diagram
- Confirms that $f_0(980)\pi$ signal is *not* an artifact of isobar parametrization

$\pi\pi$ S-Wave Amplitude in $J^{PC} = 1^{++}$ 3π Wave [arXiv:1509.00992]

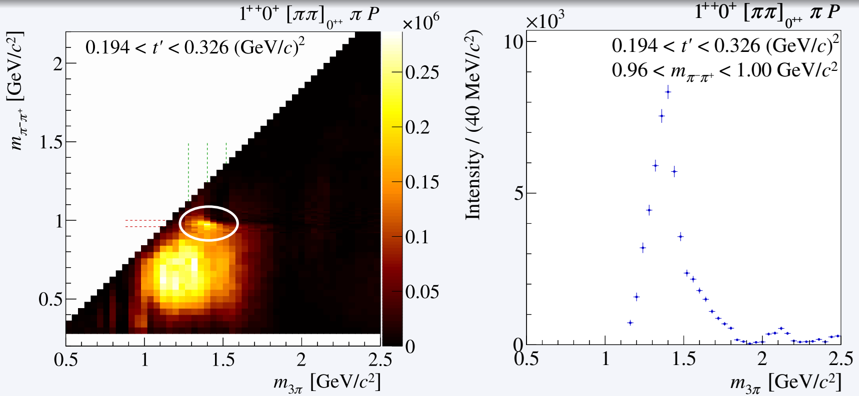

- Correlation of 3π intensity around 1.4 GeV / c^2 with $f_0(980)$
- $f_0(980)$ semicircle in Argand diagram
- Confirms that $f_0(980)\pi$ signal is *not* an artifact of isobar parametrization

$\pi\pi$ S-Wave Amplitude in $J^{PC} = 1^{++}$ 3π Wave [arXiv:1509.00992]

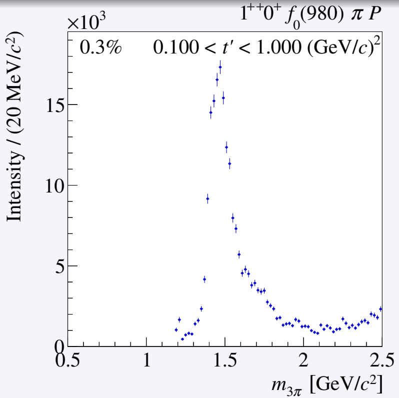

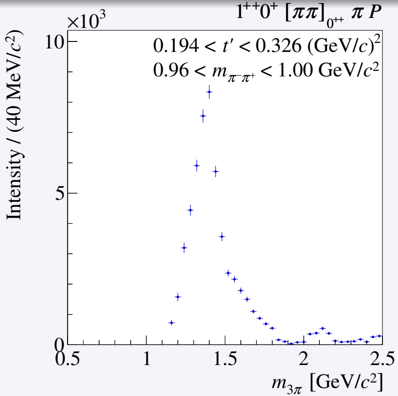

- Correlation of 3π intensity around 1.4 GeV / c^2 with $f_0(980)$
- $f_0(980)$ semicircle in Argand diagram
- Confirms that $f_0(980)\pi$ signal is *not* an artifact of isobar parametrization

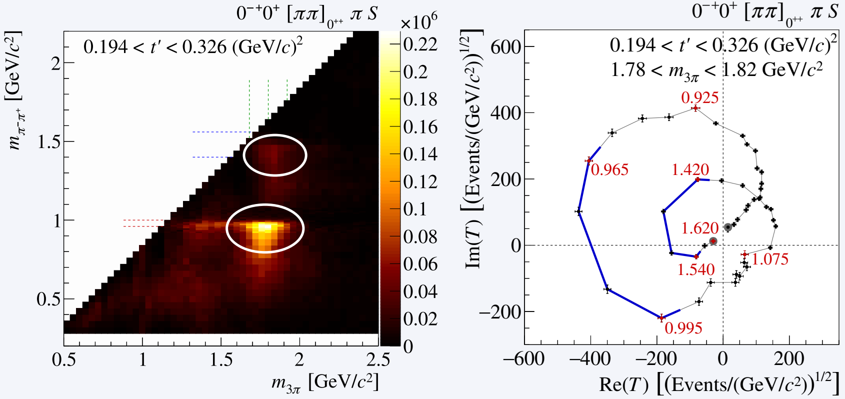

- Coupling of $\pi(1800)$ to $f_0(980)\pi$ and $f_0(1500)\pi$ decay modes